Contents lists available at SciVerse ScienceDirect

Journal of Experimental Marine Biology and Ecology
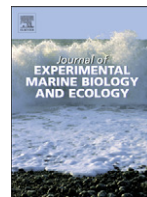
CO_2-induced ocean acidification impairs calcification in the tropical urchin *Echinometra viridis*

T. Courtney, I. Westfield, J.B. Ries *

Department of Marine Sciences, University of North Carolina at Chapel Hill, Chapel Hill, NC 27599, USA

A B S T R A C T

Atmospheric carbon dioxide (pCO_2) has risen from approximately 280 to 400 ppm since the Industrial Revolution, due mainly to the combustion of fossil fuels, deforestation, and cement production. It is predicted to reach as high as 900 ppm by the end of this century. Ocean acidification resulting from the release of anthropogenic CO_2 has been shown to impair the ability of some marine calcifiers to build their shells and skeletons. Here, we present the results of ocean acidification experiments designed to assess the effects of an increase in atmospheric pCO_2 from ca. 448 to 827 ppm on calcification rates of the tropical urchin *Echinometra viridis*. Experiments were conducted under the urchin's winter (20 °C) and summer (30 °C) water temperatures in order to identify seasonal differences in the urchin's response to ocean acidification. The experiments reveal that calcification rates decreased for urchins reared under elevated pCO_2, with the decline being more pronounced under wintertime temperatures than under summertime temperatures. These results indicate that the urchin *E. viridis* will be negatively impacted by CO_2-induced ocean acidification that is predicted to occur by the end of this century. These results also suggest that impact of CO_2-induced ocean acidification on urchin calcification will be more severe in the winter and in cooler waters.

© 2012 Elsevier B.V. All rights reserved.

1. Introduction

Atmospheric pCO_2 has increased from approximately 280 to 400 ppm since the Industrial Revolution, primarily due to the anthropogenic combustion of fossil fuels, deforestation, and cement production (IPCC Assessment 4, 2007; Keeling, 1960; Keeling et al., 2009; Neftel et al., 1985; Rahmstorf et al., 2007; Worrell et al., 2001). This post-Industrial increase in atmospheric pCO_2 has caused the pH of surface seawater to decrease by approximately 0.1 units (Raven et al., 2005). Current estimates predict that atmospheric pCO_2 could reach as high as 900 ppm by the end of this century, resulting in a decrease in seawater pH of up to 0.3–0.4 units (Brewer, 1997; Caldeira and Wickett, 2005; IPCC Assessment 4, 2007; Raven et al., 2005). Recent studies suggest that these reductions in seawater pH will impair shell and skeletal production within many calcifying marine organisms (e.g., Doney et al., 2009; Fabry et al., 2008; Iglesias-Rodriguez et al., 2008; Kleypas et al., 2006; Ries et al., 2009; Rodolfo-Metalpa et al., 2010; Wood et al., 2008).

Sea urchin tests are composed of large, optically aligned crystals of high magnesium (~5–8%) calcite and occluded glycoproteins (<0.1% by mass) that form complex, rounded vesicular structures filled with living tissue (Politi et al., 2004; Wilt, 1999, 2002). Recent investigations focused on larval urchin development and adult urchin spine regeneration report that urchin biomineralization is mediated by organic matrices (DuBois and Chen, 1989; Politi et al., 2004; Wilt, 1999, 2002), where vesicles transport protein-stabilized amorphous calcium carbonate (ACC) into a syncytium composed of primary mesenchyme cells (Politi et al., 2004; Wilt, 2002). This syncytium controls ion balance, liquid volume, and shape of the mineralization site, thereby regulating the crystallization of high-magnesium calcite into the complex framework that composes the urchin endoskeleton (DuBois and Chen, 1989; Politi et al., 2004; Wilt, 2002).

Yet despite urchins' apparently strong biomineralogical control, previous work has shown that their calcification can be strongly influenced by the physical properties of seawater (Borremans et al., 2009; Dickson, 2002; McClintock et al., 2011; Ries, 2004; Weber, 1969, 1973). The effects of seawater pH, in particular, on the growth and calcification of echinoderms have been investigated in numerous studies (e.g., Brennand et al., 2010; Gooding et al., 2009; Ries et al., 2009; Shirayama and Thornton, 2005; Wood et al., 2008). One study (Gooding et al., 2009), conducted on the sea star *Pisaster ochraceus*, found that calcified mass decreased relative to the control (380 ppm pCO_2) when the sea star was reared under acidified conditions (780 ppm pCO_2). However, total growth rates remained constant due to increased soft tissue production under acidified conditions. This same study also examined the effects of temperature on total growth rates and found that total growth

* Corresponding author at: Department of Marine Sciences, 3202 Venable Hall, CB# 3300, University of North Carolina, Chapel Hill, Chapel Hill, NC 27599, USA. Tel.: +1 919 536 9070; fax: +1 919 962 1254.
E-mail address: riesjustin@gmail.com (J.B. Ries).

decreased linearly with temperature from 21° to 5 °C at 380 ppm pCO$_2$. The study revealed no other deleterious impacts on health during the experimental period, despite the decrease in calcified mass.

Conversely, a study conducted on the brittlestar *Amphiura filiformis* revealed that calcification rates increased while rates of muscle mass production decreased when seawater was acidified from pH 8.0 to 6.8 (Wood et al., 2008), suggesting that the maintenance of elevated rates of calcification under the high-pCO$_2$ conditions came at the metabolic expense of muscle generation. A study on the effects of ocean acidification on the growth of the urchin *Echinometra mathaei* revealed a decrease in net calcification under high-pCO$_2$ conditions (modern atmospheric pCO$_2$ + 200 ppm) compared with net calcification rates under modern atmospheric pCO$_2$ (Shirayama and Thornton, 2005). Ries et al. (2009) reared the tropical urchin *Eucidaris tribuloides* and the temperate urchin *Arbacia punctulata* under pCO$_2$ levels of ca. 400, 600, 900, and 2850 ppm. They found that the tropical urchin *E. tribuloides* exhibited a 'threshold-negative' response to elevated pCO$_2$ (with the decline evident at 2850 ppm) while the temperate urchin *A. punctulata* exhibited a 'parabolic' response (i.e., calcification increased from 400 to 900 ppm pCO$_2$ and declined at 2850 ppm). These studies collectively indicate that echinoderms exhibit variable responses to moderately acidified conditions (pCO$_2$ < 900 ppm), with a more unanimous decline in health (calcification and tissue generation) when exposed to highly acidified conditions (pCO$_2$ > 900 ppm).

Here, we report on experiments investigating the effects of CO$_2$-induced ocean acidification on the reef- and rocky-substrate-dwelling tropical urchin *Echinometra viridis*, which is widely distributed throughout the Caribbean Sea, from Southern Florida to the West Indies to Venezuela (McPherson, 1969). We reared this tropical urchin under control pCO$_2$ conditions (ca. 480 ppm) and under predicted end-of-century pCO$_2$ conditions (ca. 800 ppm), under both winter (ca. 20 °C) and summer temperatures (ca. 30 °C), in order to determine how *E. viridis* may respond to end-of-century acidification during both the warm and cold season.

2. Materials and methods

2.1. Collection and acclimation

Approximately 44 specimens of *Echinometra viridis* were collected in late January 2011 off Key Largo in Southern Florida and transported to the University of North Carolina at Chapel Hill by airplane. Temperatures near the collection site ranged from ca. 15 to 33 °C in 2010 (NOAA Station KYWFl-8724580). Specimens were acclimated to laboratory conditions for ca. 45 days in a 55 gallon holding tank that contained seawater formulated at a salinity of ca. 32 and maintained at a temperature of ca. 25 °C. The acclimating urchins were fed every other day with approximately 270 mg dehydrated marine algae.

2.2. Seawater formulation

Each experimental aquarium contained 34 liters of seawater formulated at a salinity of 32.06 ± 0.02 with *Instant Ocean Sea Salt* mixed with deionized water. Deionized water was also periodically added to the experimental aquaria in order to replenish water lost due to evaporation. 250 mL seawater samples were taken weekly for analysis of dissolved inorganic carbon and total alkalinity and were replaced with ca. 32 salinity seawater.

2.3. Aquarium conditions

Four sets of three-way replicated treatments were illuminated for 10 hr/day with T8 6500°K fluorescent lighting, which generated an average irradiance (± standard error) of 884 (± 38) Lux at the base of each aquarium. The seawater in each aquarium was filtered with a hanging power filter rated at 757 L/h that utilized activated carbon

contained within a floss-filter cartridge. Each aquarium was covered with a thin, transparent plexiglass sheet. Cellophane wrap was used to seal the top of each aquarium and filtration system, which minimized evaporation and gas exchange with external air. The low-temperature treatments were circulated and cooled to 20.42 ± 0.07 °C by pumping the aquarium seawater through coiled tubes that passed through a water bath maintained at a sufficiently low temperature by an *Oceanic 1 HP Aquarium Chiller (Model 01505)*. The high-temperature seawaters were maintained at 29.93 ± 0.04 °C with 50-W heaters and were circulated within each aquarium with powerheads at 400 L/h.

2.4. Feeding

The urchins were fed to the point of satiation every other day with approximately 60 mg of dehydrated marine green algae per tank. Glass beads were used to weigh down the algal sheets on the base of the tank and the urchins were placed on top of the sheets at each feeding. Excess food was removed from the aquaria prior to the next feeding.

2.5. Experimental conditions

Urchins were reared for 60 days under three-way replicated low (ca. 480 ppm) and high (ca. 800 ppm) pCO$_2$ treatments (Table 1), which were each maintained at low (ca. 20 °C) and high temperature levels (ca. 30 °C). The actual pCO$_2$ and temperature values for the four treatments (± standard error) were: (1) 20.3 ± 0.1 °C and 524 ± 33 ppm; (2) 20.56 ± 0.09 °C and 827 ± 37 ppm; (3) 30.00 ± 0.06 °C and 448 ± 27 ppm; and (4) 29.86 ± 0.06 °C and 783 ± 45 ppm (Table 1). The high-pCO$_2$ gas was formulated by mixing compressed CO$_2$ gas with compressed air using *Aalborg* mass flow controllers. The low CO$_2$-gas was compressed air supplied to the laboratory through an in-house airline and was sourced from air outside of the laboratory building. The gases were bubbled into the aquaria via 6-in. porous ceramic airstones that were fastened to the bottom of each tank. For a given pCO$_2$ treatment, calculated pCO$_2$ levels for the lower temperature seawaters were greater than those for the higher temperature seawaters because the solubility of CO$_2$ gas in seawater increases with decreasing temperature (Weiss, 1974).

2.6. Carbonate system parameters

2.6.1. Measured parameters

Temperature within the experimental aquaria was measured every other day (Table 1) with a NIST-calibrated partial-immersion organic-filled glass thermometer. Salinity was measured every other day (Table 1) with a *YSI 3200* conductivity meter with a *YSI 3440* cell ($K = 10$) that was calibrated with seawater standards of known salinity provided by the laboratory of Prof. A. Dickson of Scripps Institute of Oceanography. Seawater pH was measured every other day (Table 1) with a *Thermo Scientific Orion 2 Star* benchtop pH meter and *Orion 9156BNWP* probe, calibrated with 7.00 and 10.01 Orion NBS buffers traceable to NIST standard reference material (for slope of the calibration curve) and with seawater standards of known pH provided by the laboratory of Prof. A. Dickson of Scripps Institute of Oceanography (for y-intercept of the calibration curve). Seawater dissolved inorganic carbon (DIC) and total alkalinity (TA) were measured weekly (Table 1) with a VINDTA 3C (*MARIANDA* corporation). Seawater DIC was measured via coulometry (*UIC 5400*) and TA was measured via closed-cell potentiometric titration.

2.6.2. Calculated parameters

Seawater pCO$_2$, pH, carbonate ion concentration ([CO$_3^{2-}$]), bicarbonate ion concentration ([HCO$_3^-$]), aqueous CO$_2$, and aragonite saturation state (Ω_A) were calculated (Table 1) with the program *CO$_2$SYS* (Lewis and Wallace, 1998), using Roy et al. (1993) values for the K_1 and K_2

Table 1
Average measured parameters: temperature, salinity, pH, total alkalinity (TA), and dissolved inorganic carbon (DIC). Average calculated parameters: pCO_2 of the mixed gases in equilibrium with the experimental seawaters [pCO_2 (gas-e)], pH, carbonate ion concentration ([CO_3^{2-}]), bicarbonate ion concentration ([HCO_3^{-}]), dissolved CO_2 ([CO_2] $_{(SW)}$), and aragonite saturation state (Ω_A). 'SE' is standard error and n is sample size.

Measured values					
Temperature	(°C)	20.3	20.6	30.0	29.9
	SE	0.1	0.1	0.1	0.1
	Range	19.3–21.2	19.9–21.6	29.5–30.6	29.3–30.4
	n	27	27	27	27
Salinity		32.00	32.07	32.12	32.07
	SE	0.03	0.02	0.06	0.04
	Range	31.60–32.40	31.80–32.40	31.00–32.90	31.60–32.60
	n	27	27	27	27
pH		8.23	8.00	8.34	8.11
	SE	0.01	0.01	0.01	0.01
	Range	8.17–8.29	7.83–8.05	8.26–8.42	8.04–8.20
	n	27	27	27	27
TA	(µM)	3383	3574	3289	3335
	SE	29	27	35	44
	Range	3157–3738	3289–3905	2785–3568	2837–3678
	n	27	27	27	27
DIC	(µM)	2979	3304	2744	2951
	SE	17	18	32	37
	Range	2785–3114	3148–3435	2367–3057	2490–3209
	n	27	27	27	27
Calculated values					
pCO_2 $_{(gas-e)}$	(ppm-v)	524	827	448	783
	SE	33	37	27	45
	Range	272–950	445–1137	240–713	479–1495
	n	27	21	27	27
pH		8.25	8.04	8.29	8.10
	SE	0.02	0.03	0.02	0.02
	Range	7.99–8.49	7.68–8.34	8.10–8.51	7.85–8.30
	n	27	27	27	27
[CO_3^{2-}]	(µM)	330	241	437	320
	SE	16	14	16	13
	Range	189–527	106–437	300–645	180–485
	n	27	27	27	27
[HCO_3^{-}]	(µM)	2632	3031	2296	2611
	SE	21	20	37	34
	Range	2444–2842	2849–3247	2016–2650	2199–2867
	n	27	27	27	27
[CO_2]$_{(SW)}$	(µM)	17	32	11	20
	SE	1	2	1	1
	Range	9–30	15–73	6–18	12–38
	n	27	27	27	27
Ω_A		5.2	3.8	7.2	5.3
	SE	0.3	0.2	0.3	0.2
	Range	3.0–8.3	1.7–6.9	5.0–10.7	3.0–8.1
	n	27	27	27	27

carbonic acid constants, the Mucci (1983) value for the stoichiometric aragonite solubility product, and an atmospheric pressure of 1.015 atm.

2.7. Estimation of net calcification rates

Calcification rates were estimated from changes in the urchins' buoyant weight between the beginning and end of the experiment (Table 2). The average initial buoyant weights ($\pm$ standard error) of the urchin specimens for the four treatments were 1358 ± 216 mg, 1521 ± 456 mg, 1203 ± 142 mg, and 1232 ± 124 mg and were not significantly different amongst treatments.

Echinometra viridis specimens were weighed at the beginning and end of the experiment via the buoyant weight method (Fig. 1; see Ries et al., 2009, for details regarding application of this method to urchins). A *Cole Parmer Symmetry PR 410* bottom loading electronic balance was suspended over a 38-l aquarium containing seawater that was maintained at a constant temperature, salinity, and depth. An aluminum wire attached to a small basket was suspended from the bottom-loading hook of the scale so that the basket was approximately mid-

depth in the aquarium. Urchin specimens were loaded into the basket and their buoyant weights recorded.

After completion of the experiment, the urchins were dried in an oven at 66 °C for five hours and massed to determine their dry weights. The buoyant and dry weights of the urchin tests were highly linearly correlated ($R^2 = 0.9978$) with a *y*-intercept close to zero (Fig. 1):

$$\text{Dry Weight (mg)} = 1.59 \times \text{Buoyant Weight (mg)} + 46 \qquad (1)$$

This equation was used to estimate initial dry weights for the urchins from their initial buoyant weights (Table 2). Net calcification rates are expressed as percent change in buoyant weight (Fig. 2).

2.8. Statistical analysis

We used a split plot design mixed-effects model with random intercepts varying by aquarium to model the effects of the two controlled parameters in the experiment, pCO_2 and temperature, on percent change in buoyant weight of *E. viridis* specimens over the 60-day experiment. This approach was particularly useful as it allowed us to isolate the effects of temperature and CO_2 on calcification rate, despite the fact that the two parameters are not truly independent (temperature of seawater influences the solubility of CO_2 in seawater). The statistical package *R 2.15.1 GUI 1.52 Leopard build 64-bit (6188)* was used to determine and analyze the model that best describes the effects of temperature and pCO_2 on the percent change in buoyant weight of the urchins and to identify any interactive effects between these two parameters. This process is based on the Akaike Information Criterion (AIC), which scales the estimated difference between the model equation and the actual equation for the percent change in buoyant weight, thereby rendering models with smaller AIC values more accurate (Burnham and Anderson, 2002). This criterion is based on the goodness of fit of the data combined with a correction term that slightly increases the AIC value with increasing numbers of predictors, optimizing the model with the lowest AIC value for both fit and simplicity (Burnham and Anderson, 2002).

Initially, single variable models involving only pCO_2 and temperature were analyzed (Table 4). The model incorporating pCO_2 yielded the lowest AIC value and was therefore chosen as the first predictor for the data (Table 4). The addition of temperature to the pCO_2 model yielded an equation with a lower AIC value than the single variable pCO_2 model and was therefore added to the regression (Table 4). A variable expressing the combined, interactive effects of temperature and pCO_2 was then added to the equation; however, adding this variable to the model yielded a greater AIC value and failed to yield significant ($p < 0.05$) predictors, and was thus not included in the model (Table 4).

Therefore, the additive model that included the independent effects of pCO_2 and T proved to be the most predictive model. The summary of this model (Table 5) reveals that both temperature and pCO_2 are significant ($p < 0.05$) predictors of urchin calcification rate.

3. Results

3.1. Mortalities

There were a total of eight mortalities throughout the experiment; however, survivorship was not significantly correlated with temperature (ANOVA, $p = 0.4466$) or pCO_2 (ANOVA, $p = 0.8648$). Furthermore, all of these mortalities occurred within the first twenty days of the experiment.

3.2. Calcification rates

The average percent change in buoyant weight ($\pm$ standard error) of the urchins over the 60-day experiment for the 20.3 °C–524 ppm, 30.0 °C–448 ppm, 20.6 °C–827 ppm, and 29.9 °C–783 ppm treatments were 1.3 ± 3.9, 15.9 ± 4.1, -14.6 ± 7.5, and 3.9 ± 4.7 %, respectively

Table 2
Initial and final measured buoyant weights, %-change in buoyant weight, initial dry weight (estimated from initial buoyant weight via the buoyant-dry weight regression, Fig. 1), final measured dry weight, and %-change in dry weight of the urchins reared under the experimental conditions.

Treatment	Initial buoyant weight (mg)	Final buoyant weight (mg)	% Change buoyant weight	Initial dry weight (mg)	Final dry weight (mg)	% Change dry weight
20.3 °C 524 ppm-v	2345	2368	0.98	3775	3794	0.50
	695	728	4.75	1151	1196	3.91
	1250	1051	−15.92	2034	1680	−17.40
	1380	1634	18.41	2240	2798	24.91
	700	686	−2.00	1159	1081	−6.73
	1617	1694	4.76	2617	2776	6.08
	1520	1494	−1.71	2463	2409	−2.19
20.6 °C 827 ppm-v	783	856	9.32	1291	1339	3.72
	1305	802	−38.54	2121	1365	−35.64
	1344	1212	−9.82	2183	1982	−9.21
	834	585	−29.86	1372	967	−29.52
	1109	884	−20.29	1809	1424	−21.28
	3750	3816	1.76	6009	6090	1.35
30.0 °C 448 ppm-v	800	1042	30.25	1318	1720	30.50
	1135	1407	23.96	1851	2302	24.37
	1073	1071	−0.19	1752	1807	3.14
	1240	1548	24.84	2018	2456	21.70
	1975	2117	7.19	3186	3438	7.91
	945	1072	13.44	1549	1746	12.72
	1252	1396	11.50	2037	2221	9.03
29.9 °C 783 ppm-v	975	1219	25.03	1596	1991	24.75
	872	972	11.47	1432	1580	10.34
	1449	1585	9.39	2350	2617	11.36
	895	911	1.79	1469	1585	7.90
	1147	1167	1.74	1870	1880	0.53
	1833	1449	−20.95	2960	2357	−20.37
	1113	1054	−5.30	1816	1717	−5.45
	1573	1697	7.88	2547	2779	9.11

(Table 3, Fig. 2). Calcification rates are negatively correlated with $p\mathrm{CO_2}$ (Fig. 2A–B; ANOVA, $p = 0.02231$) and positively correlated with temperature (Fig. 2C–D; ANOVA, $p = 0.02946$).

3.3. Model building

The coefficients and intercepts of the split plot design mixed-effects model (Table 5) yield the following equation, which predicts with 97.5% confidence the percent change in urchin buoyant weight

Fig. 1. Plot of final buoyant weight vs. final dry weight for the studied urchins. The strong linear correlation ($R^2 = 0.9978$) between final buoyant weight and final dry weight allows percent change in buoyant weight to be used as a proxy for the urchin's net calcification rate.

as a function of the fixed-effects of temperature and $p\mathrm{CO_2}$, as observed throughout the 60-day experiment:

$$\%-\text{Change Buoyant Weight} = 1.58 \pm 1.26 \times \mathrm{T}\ (°\mathrm{C}) - 0.048 \pm 0.036 \times p\mathrm{CO_2}(\mathrm{ppm-v}) - 7.8 \pm 43.0 \quad (2)$$

4. Discussion

Our results indicate that *Echinometra viridis* specimens exposed to high $p\mathrm{CO_2}$ treatments exhibit lower calcification rates than *E. viridis* exposed to lower, control $p\mathrm{CO_2}$ treatments (Table 5, Fig. 2A-B). Urchins reared in ca. 20 °C treatments also exhibit lower calcification rates than those reared in ca. 30 °C treatments (Table 5, Fig. 2A-B). Urchins reared in the 20.6 °C–827 ppm treatment, which is predicted to occur during winter months by the end of this century (IPCC Assessment 4, 2007), exhibited the most significant decrease in buoyant weight (−14.6 ± 7.5 %, Table 3, Fig. 2). Notably, under these conditions, the urchins exhibited net loss of calcified material between the beginning and end of the experiment. This suggests that given sufficient time, this species of urchin could lose much or all of its calcified material under conditions that are predicted during the winter months for the end of this century. Although calcification rates in the 29.9 °C–783 ppm treatment were less than those of urchins reared under the 30.0 °C–448 ppm control treatment, the urchins still maintained positive calcification rates (3.9 ± 4.7 %) under the high-$p\mathrm{CO_2}$, high-temperature treatment that is predicted during the summer months for the end of this century (Table 3). This suggests that under $\mathrm{CO_2}$ partial pressures predicted for the end of the century, net positive calcification would still occur in summer, but a net loss of calcified material would occur in winter. A key question is how net calcification in the summer and net loss of calcified material in the winter will balance out on an annual basis, as this may determine whether this species of urchin can grow and/or maintain its spines and test year-to-year under conditions predicted for the end of this century. However, this balance depends upon the duration and intensity of the
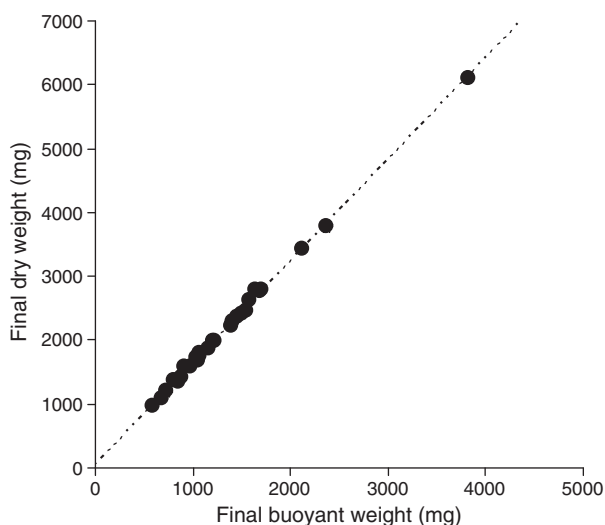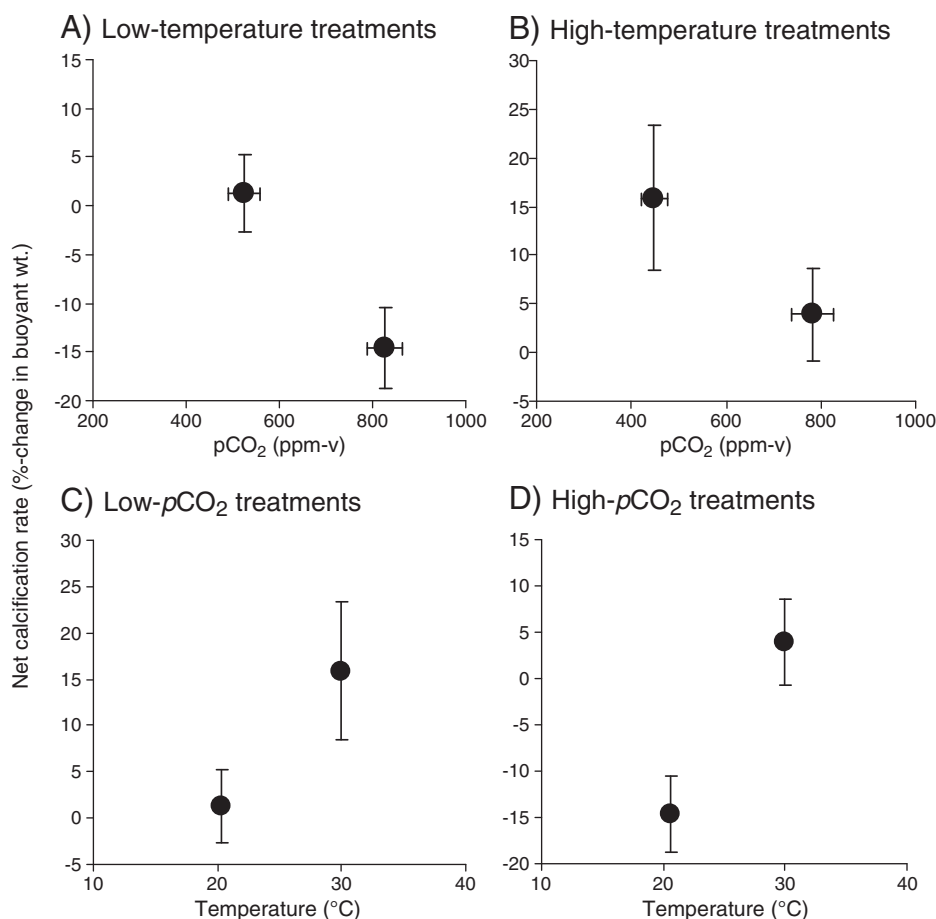
Fig. 2. Temperature vs. net calcification rate for the low (A) and high (B) pCO₂ treatments; pCO₂ vs. net calcification rate for the low (C) and high (D) temperature treatments. Error bars represent standard error.

winter and summer seasons and, therefore, cannot be assessed with the data at hand.

Our results (Table 5) also suggest that the negative effects of ocean acidification on urchin calcification will be first experienced and/or exacerbated in cooler waters (e.g., at higher latitudes, along zones of upwelling, and in areas influenced by cold-water currents). Likewise, the urchins' positive calcification response to warmer temperatures (Table 5) raises the possibility that the apparently deleterious effects of ocean acidification on this species may be partially mitigated by warming of the oceans that is predicted to accompany elevated levels of atmospheric pCO_2. However, this study investigated temperatures (ca. 20, 30 °C) that occur annually within the Florida Key waters from which these specimens were collected. If temperatures continue to rise beyond the natural range for this species, it is possible that temperature could begin to have a negative effect on urchin calcification, as opposed to the positive effect observed in the present

study—potentially rendering this species of urchin even more susceptible to the effects of CO_2-induced ocean acidification. Additional experiments, ideally conducted at temperatures greater than 30 °C, are needed to examine these potential interactions.

Our results indicate that calcification rates for the urchin *E. viridis* decrease under CO_2-acidified conditions and increase under warmer

Table 4
Effects of using (1) no predictors ('<none>'), (2) only temperature (*T*), (3) only pCO_2 ('pCO_2'), (4) both pCO_2 and temperature ('pCO_2+T'), and (5) pCO_2, temperature, and the combined interactive effects of temperature and pCO_2 ('pCO_2+T+T:pCO_2') as predictors on model AIC results.

Predictors	AIC
<none>	103.71
T	99.75
pCO_2	99.14
pCO_2+T	93.51
pCO_2+T+T:pCO_2	94.58

Table 3
Mean net calcification rates (%-change in buoyant weights), standard error (SE), range, and sample size (n) of urchins reared under experimental temperature and pCO_2 conditions.

Temperature (°C)	pCO₂ (ppm-v)	Calcification (wt%/60-day AVG)	SE	Range	n
20.3	524	1.3	3.9	−15.9 to 18.4	7
30.00	448	15.9	4.1	−0.2 to 30.3	7
20.56	827	−14.6	7.5	−38.5 to 9.3	6
29.86	783	3.9	4.7	−21.0 to 25.0	8

Table 5
Summary data for the best AIC model: intercept ('Intercept') and predicted slopes for temperature (*T*) and pCO_2 of the model equation. 'SE' is standard error.

Predictor	Value	SE	t-Value	p-Value
Intercept	−7.8	19.0	−0.41	0.692
pCO₂	−0.048	0.016	−2.98	0.020
T	1.58	0.56	2.83	0.016

temperatures (Table 5). This is consistent with the observations that calcification by the sea star *Pisaster ochraceus* (Gooding et al., 2009) and the urchin *Echinometra mathaei* (Shirayama and Thornton, 2005) decreases under high-pCO_2 conditions. Our observations that calcification by *E. viridis* decreased as pCO_2 was elevated to ca. 800 ppm contrasted with observations by Ries et al. (2009) that rates of calcification in the tropical and temperate urchins *Eucidaris tribuloides* and *Arbacia punctulata* remained relatively constant and increased, respectively, as pCO_2 was elevated from ca. 400 to 900 ppm. Nevertheless, our results agree with Ries et al. 's (2009) general conclusion that the response of calcifying marine organisms to CO_2-induced ocean acidification is variable and complex. Our results also contrast with the results of a prior study showing that calcification rates of the brittle star *Amphiura filiformis* increased under CO_2-acidified conditions (Wood et al., 2008). However, the same study found that these brittle stars exhibit a reduction in muscle mass under CO_2-acidified conditions. Future work should investigate whether muscle mass of *E. viridis* also decreases under acidified conditions.

Ocean acidification experiments conducted on echinoderm reproduction, larval growth, and larval survival reveal responses similar to those observed in the present study. Laboratory experiments have revealed that a decrease in seawater pH from 8.1 to 7.7 reduced reproductive success of the urchin *Heliocidaris erythrogramma* by 25% (Havenhand et al., 2008). A study conducted on the urchin *Tripneustes gratilla* during its first 5 days of life revealed a decrease in post oral arm length at 24 °C compared to 27 °C and a decrease in post oral arm length at pH of 7.60 compared to 8.15 (Brennand et al., 2010). Over the range of values investigated, the decrease in water temperature had a more negative impact on urchin larval development than the decrease in seawater pH. Larval brittle stars (*Ophiothrix fragilis*) reared in the laboratory for 8 days under seawater acidified to pH of 7.9 experienced 100% mortality compared to mortality rates of only 30% under a pH of 8.1 (Dupont et al., 2008). Although these results are generally consistent with the results of the present experiment on the adult tropical urchin *E. viridis*, additional experiments are needed to determine whether the effects of acidification and warming on *E. viridis* larvae also conform to this pattern.

5. Conclusions

The present study reveals that calcification rates for the tropical urchin *E. viridis* increase with warming from ca. 20 to 30 °C and decrease with seawater acidification that accompanies an increase in atmospheric pCO_2 from ca. 448 to 827 ppm (Table 5). This suggests that CO_2-induced ocean acidification predicted to occur by the end of the 21st century will reduce calcification rates within this urchin. These results also underscore the importance of seasonal variability in this urchin's response to ocean acidification: for pCO_2 predicted for the end of the century, net loss of calcified material is predicted to occur during the winter while net positive calcification is predicted to occur during the summer. These results also raise the possibility that the effects of ocean acidification on urchins will be more severe in cooler waters and that the negative effects of ocean acidification on the urchin *E. viridis* may be partially offset by warming of the oceans that is predicted to accompany elevated atmospheric pCO_2. Future studies should investigate the effects of CO_2-induced ocean acidification on tissue growth and larval development of *E. viridis*, explore the effects of temperatures that span a broader range than those investigated in the present study, and evaluate the broader ecological impacts of impaired calcification within the tropical urchin *E. viridis*.

Acknowledgements

References

Borremans, C., Hermans, J., Baillon, S., André, L., Dubois, P., 2009. Salinity effects on the Mg/Ca and Sr/Ca in starfish skeletons and the echinoderm relevance for paleoenvironmental reconstructions. Geology 37, 351–354.

Brennand, H., Soars, N., Dworjanyn, S., Davis, A., Byrne, M., 2010. Impact of ocean warming and ocean acidification on larval development and calcification in the sea urchin *Tripneustes gratilla*. PLoS One 5, e11372.

Brewer, P.G., 1997. Ocean chemistry of the fossil fuel CO_2 signal: the haline signal of "business as usual". Geophys. Res. Lett. 24, 1367–1369.

Burnham, K., Anderson, D., 2002. Model Selection and Multimodel Inference: A Practical Information-Theoretic Approach. Springer Verlag, pp. 60–64.

Caldeira, K., Wickett, M.E., 2005. Ocean model predictions of chemistry changes from carbon dioxide emissions to the atmosphere and ocean. J. Geophys. Res. 110, C09S04.

Dickson, J.A.D., 2002. Fossil echinoderms as monitor of the Mg/Ca ratio of Phanerozoic oceans. Science 298, 1222–1224.

Doney, S.C., Fabry, V.J., Feely, R.A., Kleypas, J.A., 2009. Ocean acidification: the other CO_2 problem. Ann. Rev. Mar. Sci. 1, 169–192.

Dubois, P., Chen, C.P., 1989. Calcification in echinoderms. In: Jangoux, M., Lawrence, J.M. (Eds.), Echinoderm studies, vol. 3. A.A. Balkema, Rotterdam, pp. 109–178.

Dupont, S., Havenhand, J., Thorndyke, W., Peck, L., Thorndyke, M., 2008. Near-future level of CO_2-driven ocean acidification radically affects larval survival and development in the brittlestar *Ophiothrix fragilis*. Mar. Ecol. Prog. Ser. 373, 285–294.

Fabry, V.J., Seibel, B.A., Feely, R.A., Orr, J.C., 2008. Impacts of ocean acidification on marine fauna and ecosystem processes. ICES J. Mar. Sci. 65, 414–432.

Gooding, R., Harley, C., Tang, E., 2009. Elevated water temperature and carbon dioxide concentration increase the growth of a keystone echinoderm. PNAS 106, 9316–9321.

Havenhand, J., Buttler, F., Thorndyke, M., Williamson, J., 2008. Near-future levels of ocean acidification reduce fertilization success in a sea urchin. Curr. Biol. 18, R651–R652.

Iglesias-Rodriguez, M.D., Halloran, P.R., Rickaby, R.E.M., Hall, I.R., Colmenero-Hidalgo, E., Gittins, J.R., Green, D.R.H., Tyrrell, T., Gibbs, S.J., von Dassow, P., Rehm, E., Armbrust, E.V., Boessenkool, K.P., 2008. Phytoplankton calcification in a high-CO_2 world. Science 320, 336–340.

IPCC Assessment 4, 2007. Carbon Dioxide: Projected emissions and Concentrations. http://www.ipcc-data.org/ddc_co2.html.

Keeling, C.D., 1960. The concentration and isotopic abundances of carbon dioxide in the atmosphere. Tellus 12, 200–203.

Keeling, R.F., Piper, S.C., Bollenbacher, A.F., Walker, J.S., 2009. Atmospheric CO_2 records from sites in the SIO air sampling network. Trends: A Compendium of Data on Global Change. Carbon Dioxide Information Analysis Center, Oak Ridge National Laboratory, U.S. Department of Energy, Oak Ridge, Tennessee, USA (http://cdiac.ornl.gov/trends/co2/sio-mlo.html).

Kleypas, J.A., Feely, R.A., Fabry, V.J., Langdon, C., Sabine, C.L., Robbins, L.L., 2006. Impacts of ocean acidification on coral reefs and other marine calcifiers: a guide for future research. Report of a workshop held 18– 20 April 2005, St Petersburg, FL, sponsored by NSF, NOAA, and the US Geological Survey (88 pp.).

Lewis, E., Wallace, D.W.R., 1998. CO2SYS: Program developed for CO_2 system calculations, ORNL/CDIAC-105. Carbon Dioxide Information Analysis Center, Oak Ridge National Laboratory, U.S. Department of Energy, Oak Ridge, Tennessee.

McClintock, J.B., Amsler, M.O., Angus, R.A., Challener, R.C., Schram, J.B., Amsler, C.D., Mah, C.L., Cuce, J., Baker, B.J., 2011. The Mg-calcite composition of Antarctic echinoderms: important implications for predicting the impacts of ocean acidification. J. Geol. 119, 457–466.

McPherson, B., 1969. Studies on the biology of the tropical urchins, *Echinometra lucunter* and *Echinometra viridis*. Bull. Mar. Sci. 19, 194–213.

Mucci, A., 1983. The solubility of calcite and aragonite in seawater at various salinities, temperatures, and one atmosphere total pressure. Am. J. Sci. 283, 780–799.

Neftel, A., Moor, E., Oeschger, H., Stauffer, B., 1985. Evidence from polar ice cores for the increase in atmospheric CO_2 in the past two centuries. Nature 315, 45–47.

NOAA Station KYWFI-8724580. NOAA National Data Buoy Center http://www.ndbc.noaa.gov/download_data.php?filename=kywf1h2010.txt.gz&dir=data/historical/stdmet/.

Politi, Y., Arad, T., Klein, E., Weiner, S., Addadi, L., 2004. Sea urchin spine calcite forms via a transient amorphous calcium phase. Science 306, 1161–1164.

Rahmstorf, S., Cazenave, A., Church, J.A., Hansen, J.E., Keeling, R.F., Parker, D.E., Somerville, R.C.J., 2007. Recent climate observations compared to projections. Science 316, 709.

Raven, J., Caldeira, K., Elderfield FRS, H., Hoegh-Guldberg, O., Liss, P., Riebessel, U., Shepherd FRS, J., Turley, C., Watson FRS, A., Heap, R., Banes, R., Quinn, R., 2005. Ocean Acidification due to Increasing Atmospheric Carbon Dioxide. The Royal Society (60 pp.).

Ries, J.B., 2004. Effect of ambient Mg/Ca ratio on Mg fractionation in calcareous marine invertebrates: a record of the oceanic Mg/Ca ratio over the Phanerozoic. Geology 32, 981–984.

Ries, J.B., Cohen, A.L., McCorkle, D.C., 2009. Marine calcifiers exhibit mixed responses to CO_2-induced ocean acidification. Geology 37, 1131–1134.

Rodolfo-Metalpa, R., Martin, S., Ferrier-Pages, C., Gattuso, J.P., 2010. Response of the temperate coral *Cladocora caespitosa* to mid- and long-term exposure to pCO_2 and temperature levels projected for the year 2100 AD. Biogeosciences 7, 289–300.

Roy, R.N., Roy, L.N., Vogel, K.M., Porter-Moore, C., Pearson, T., Good, C.E., Millero, F.J., Campbell, D.M., 1993. The dissociation constants of carbonic acid in seawater at salinities 5 to 45 and temperatures 0 to 45 °C. Mar. Chem. 44, 249–267.

Shirayama, Y., Thornton, H., 2005. Effect of increased atmospheric CO_2 on shallow water marine benthos. J. Geophys. Res. 110, C09S08.

Weber, J.N., 1969. The incorporation of magnesium into the skeletal calcites of echinoderms. Am. J. Sci. 267, 537–566.

Weber, J.N., 1973. Temperature dependence of magnesium in echinoid and asteroid skeletal calcite: a reinterpretation of its significance. J. Geol. 81, 543–556.

Weiss, R.F., 1974. Carbon Dioxide in water and seawater: the solubility of a non-ideal gas. Mar. Chem. 2, 203–215.

Wilt, F.H., 1999. Matrix and mineral in the sea urchin larval skeleton. J. Struct. Biol. 126, 216–226.

Wilt, F.H., 2002. Biomineralization of the spicules of sea urchin embryos. Zoolog. Sci. 19, 253–261.

Wood, H., Spicer, J., Widdicombe, S., 2008. Ocean acidification may increase calcification rates, but at a cost. Proc. R. Soc. B 275, 1767–1773.

Worrell, E., Price, L., Martin, N., Hendriks, C., Meida, L.O., 2001. Carbon dioxide emissions from the global cement industry. Annu. Rev. Energy Environ. 26, 303–329.